tion, colony purification, and cosmid DNA isolation were performed as described (*11*).
13. M. A. Behlke, H. S. Chou, K. Huppi, D. Y. Loh, *Proc. Natl. Acad. Sci. U.S.A.* **83**, 767 (1986).
14. G. Sim and A. Augustin, *Cell* **42**, 89 (1985); M. A. Behlke *et al.*, *J. Exp. Med.* **165**, 257 (1987).
15. G. F. Carle *et al.*, *Science* **232**, 65 (1986).
16. C. L. Smith *et al.*, *Methods Enzymol.*, in press.
17. High molecular weight DNA from BALB/c 3T3 fibroblasts was prepared in agarose blocks and digested with restriction enzymes according to the protocols of Carle *et al.* (*15*) and of Smith *et al.* (*16*). Restricted DNA samples were separated in a standard horizontal gel electrophoresis apparatus at 7 V/cm with the use of a programmable power inverter (Green Mountain Lab Supply). The power inverter was programmed as follows: initial forward time 1.0 second, forward increment 0.4 second, initial reverse time 0.5 second, and reverse increment 0.1 second, with a return to the initial settings after every 100 cycles of forward-reverse. Electrophoresis was performed for 14 to 16 hours at 15°C. Yeast chromosomes and a λ phage ladder were included as size markers. Separated DNA fragments were then hybridized directly in the gel as described previously (*10*).
18. G. D. Yancopoulos *et al.*, *Nature (London)* **311**, 727 (1984); G. E. Wu and C. J. Paige, *EMBO J.* **5**, 3475 (1986); R. M. Perlmutter, J. F. Kearney, S. P. Chang, L. E. Hood, *Science* **227**, 1597 (1985).
19. R. D. Garman, J. Ko, C. D. Vulpe, D. H. Raulet, *Proc. Natl. Acad. Sci. U.S.A.* **83**, 3987 (1986).
20. W. Born, J. Yagüe, E. Palmer, J. Kappler, P. Marrack, *ibid.* **82**, 2925 (1985).
21. M. G. Reth and F. W. Alt, *Nature (London)* **312**, 418 (1984).
22. G. D. Yancopoulos, T. K. Blackwell, H. Shuh, L. Hood, F. W. Alt, *Cell* **44**, 251 (1986).
23. Y. Kurosawa *et al.*, *Nature (London)* **290**, 565 (1981); A. Alessandrini, J. H. Pierce, D. Baltimore, S. V. Desiderio, *Proc. Natl. Acad. Sci. U.S.A.* **84**, 1799 (1987).
24. J. Goverman *et al.*, *Cell* **40**, 859 (1985).
25. J. Kappler, *et al.*, *ibid.* **49**, 263 (1987).
26. H. S. Chou *et al.*, *EMBO J.* **5**, 2149 (1986).
27. After submission of this manuscript, reports consistent with the direct deletional model have appeared: S. Fujimoto and H. Yamagishi, *Nature (London)* **327**, 242 (1987); K. Okazaki, D. D. Davis, H. Sakano, *Cell* **49**, 477 (1987).
28. We thank G. Carle, M. Olson, and M. R. Pozzi for advice on field-inversion gel electrophoresis, S. Anderson and M. Louie for critical comments on the manuscript, and D. London for manuscript preparation. This work was supported by funds from Howard Hughes Medical Institute (to D.D.C. and D.Y.L.) and Medical Scientist Training Grant GM07067 (to Washington University; H.S.C.).

18 May 1987; accepted 9 July 1987

Nuclear Reassembly Excludes Large Macromolecules

JOEL A. SWANSON AND PAUL L. MCNEIL

Interphase nucleus and cytoplasm are distinct compartments, whose soluble macromolecular contents mix when the nuclear envelope disassembles at mitosis. To determine how their interphase identities are reestablished, fibroblasts were loaded with fluorescent dextrans and then allowed to divide. Large dextrans (molecular weight of 40,000 or more) were excluded from condensed mitotic chromosomes and from newly formed, postmitotic interphase nuclei. Therefore, postmitotic reassembly of the nucleus as a compartment distinct from cytoplasm occurs by exclusion not only of organelles but also of soluble macromolecules. This might occur by exclusion of macromolecules from condensed chromatin throughout mitosis and completion of nuclear envelope assembly before nuclear expansion.

DURING MITOSIS THE NUCLEAR ENvelope of metazoan cells disassembles, and nucleoplasm mixes with cytoplasm. Yet interphase nucleoplasm and cytoplasm are distinct compartments, whose separate identities are maintained in part by the integrity of the nuclear envelope. Pores in the nuclear envelope provide a size-selective barrier to diffusion, confining many macromolecules (*1*) and organelles to the cytoplasm. Some large proteins are selectively concentrated in the nucleus (*2*), probably by specific transport or trapping mechanisms. Others, such as tubulin, are predominantly cytoplasmic (*3*). It is not known how, after mitosis, the distinct chemical identities of interphase nucleus and cytoplasm are reestablished. We examined this question by characterizing qualitatively and quantitatively the nucleocytoplasmic distribution of large fluorescent dextrans, initially confined predominantly to the cytoplasm, in cells that have undergone mitosis.

Dextrans labeled with fluorescein isothiocyanate (FDx) are highly water soluble molecules of low charge density that appear not to interact significantly with intracellular components or to affect cell viability (*4*). Moreover, they are available in various size ranges and are therefore useful as probes of the nucleocytoplasmic distribution of soluble macromolecules (*5*).

Dextrans were loaded into fibroblast (Swiss 3T3) cytoplasm by a modification of the scrape-loading technique (*6*). We denuded zones of cells from a monolayer by scratching the culture substratum with a sharp instrument (*7*). When the monolayer was wounded by scratching in the presence of large macromolecules such as FDx or Texas Red–labeled dextran (TRDx), many of the cells remaining on the substratum and lining the denuded zone were rendered fluorescent (Fig. 1); that is, they were loaded with exogenous molecules present during the culture wounding. Cells lining such wounds migrate into the denuded zone where DNA synthesis and mitosis are then initiated (*8*). We observed that loaded cells retained fluorescent dextrans for up to 48 hours, migrated into the denuded region, and divided, confirming for loaded cells these earlier observations of viability of cells bordering a wound. Therefore, by means of this "scratch-loading" procedure we were able to introduce the dextran probes into cell cytoplasm and, at the same time and in the same cells, to induce cell division. Scratch-loading, like microinjection and scrape-loading, relies on transient disruption of the plasma membrane. In all these methods, resealing of plasma membrane is evidenced by prolonged retention or exclusion of soluble dyes. More rigorous, long-term indications of cell health are movement and division. Scratch-loaded cells, like scrape-loaded (*6*) and microinjected cells, fulfill all these criteria. Moreover, the nuclear envelope permeability in undivided cells loaded by scratching was similar to that reported for microinjected cells (*5*). Scratch-loading should find many applications in cell biology, as it is a simple and rapid alternative to microinjection that requires only a small volume of dissolved macromolecules to be loaded.

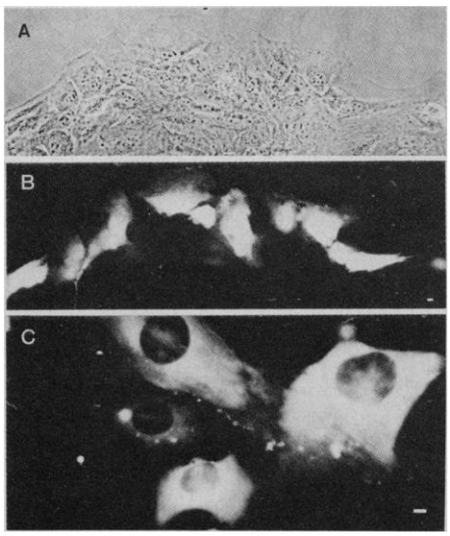

Fig. 1. Swiss 3T3 fibroblasts, 60 minutes after scratch-loading with fluorescent dextrans. (**A**) Phase-contrast images of cells bordering a denuded zone. (**B**) Fluorescein fluorescence image of cells in (A) that were scratch-loaded in the presence of FDx10, showing inclusion in the nucleus of this 10,000 molecular weight dextran. (**C**) Fluorescein fluorescence of cells scratch-loaded in the presence of FDx150, with exclusion from the nucleus of this 150,000 molecular weight dextran. Scale bars, 5 μm.

Department of Anatomy and Cellular Biology, Harvard Medical School, Boston, MA 02115.

As expected from results of work on microinjected cells (*5*), we observed that the nuclei of undivided interphase cells admitted dextrans of an average molecular weight of 4,100 and 10,000, but excluded those of average molecular weight of 40,000 or more (Fig. 1). Surprisingly, in cells that had divided after scratch-loading, nuclei continued to exclude large dextrans. In postmitotic daughter cells loaded with a mixture of TRDx10 (TRDx of average molecular weight 10,000) and FDx70 (FDx of average molecular weight 70,000) (*9*), nuclei and cytoplasm both contained TRDx10, but FDx70 was confined to the cytoplasm (Fig. 2). In mitotic cells, the region of the mitotic spindle contained dextrans of all sizes (Fig. 2). Interpretation of these images was complicated because most fibroblasts are highly rounded during mitosis. However, in less rounded specimens of mitotic fibroblasts, and in mitotic PtK2 cells, which remain flattened throughout mitosis, it was evident that large dextrans were present in the spindle but excluded from the condensed chromosomes (Fig. 3).

To quantify and extend our observation

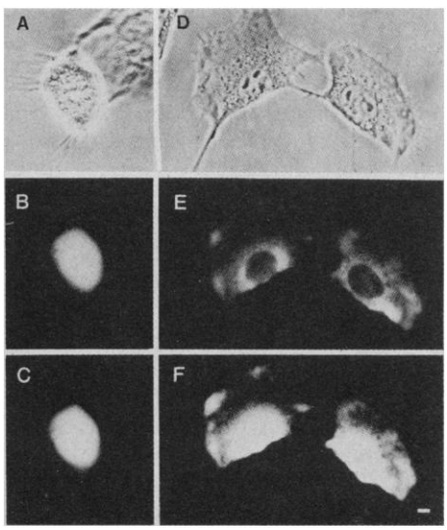

Fig. 2. A mitotic Swiss 3T3 cell (**A**, **B**, and **C**) and two postmitotic daughters (**D**, **E**, and **F**). (A) Phase-contrast image of a mitotic fibroblast. (B) Fluorescein fluorescence of FDx70 in the mitotic cell of (A). Some exclusion of the dextran is detectable in the region of the condensed chromosomes. (C) Rhodamine fluorescence of TRDx10 in the cell shown in (A). (D) Phase-contrast image of two postmitotic daughters, showing residual cytoplasmic connection. (E) Fluorescein fluorescence of FDx70 in the daughters of (D). (F) Rhodamine fluorescence of TRDx10 in the daughters of (D). The nuclear regions of the cells are thicker than the cell margins. Consequently, these regions have a greater path length, contain more TRDx, and appear more fluorescent. These images were recorded 24 hours after scratch-loading of the cells in a mixture of FDx70 and TRDx10. The scale bar represents 5 μm, the diameter of the microscope aperture used for quantitative measurements.

that reforming nuclei exclude large dextrans, we measured photometrically the fluorescence intensities of TRDx10 and FDx over the nucleus and over cytoplasm by using an aperture to restrict light collection from the fluorescent cells to a 5-μm-diameter spot (*10*). The TRDx10 served as a fluorescence reference for the cytoplasmic and nuclear space that was accessible to small dextrans, and it allowed a correction for the differences in fluorescence resulting from variation in cell thickness. From these measurements we calculated the following ratio, which we call an index of exclusion: $(FDx_{nuc})\ (TRDx_{cyt})/(FDx_{cyt})\ (TRDx_{nuc})$. An index value of 1.0 indicates that FDx and TRDx exhibit that same relative distribution between nucleus and cytoplasm; a value of less than 1.0 indicates exclusion of FDx from the nucleus (*11*).

Figure 4A shows that the indices of nuclear exclusion for FDx70 were nearly equivalent in undivided and postmitotic interphase cells, and that both were less than 1.0. This confirmed the qualitative observation that large dextrans were excluded from the reassembling nucleus. The index of exclusion measured over the spindle apparatus of mitotic cells was 1.022 ± 0.10 (SD, n = 10), indicating that at this level of resolution (5 μm), there was mixing of the large and small dextrans. No nuclear exclusion of FDx4 was detected in interphase cells (Fig. 4B).

We next measured indices of exclusion for dextrans of a wide range of molecular weights. In both premitotic and postmitotic (daughter) interphase cells, the index of exclusion equaled or slightly exceeded 1.0 for FDx4 and FDx10, and was less than 1.0 for FDx40, FDx70, and FDx150, indicating nuclear exclusion of the larger dextrans (Fig. 4C). The near identity of the indices of exclusion measured from pre- and postmitotic cells suggests that the mechanism that excludes large dextrans from the reassembling nucleus is at least as effective as the barrier characteristic of the interphase cell. A limit of exclusion of a molecular weight of about 40,000 is comparable to that calculated for other intact, interphase nuclei (*5*).

Feldherr (*12*) examined nuclear envelope permeability in *Amoeba proteus* before and after cell division. He noted that during and just after mitosis large colloidal gold molecules accumulated within nuclei. Because colloidal gold was concentrated in nuclei, presumably as a result of binding, it was difficult to establish the sizes of soluble molecules admitted into, or excluded from, the reassembling nucleus during mitosis.

How might exclusion of high molecular weight dextrans from the reforming nucleus be achieved? Mitotic chromosomes are highly condensed and appear to exclude large dextrans. Such exclusion could be the result of a compact, chromosomal structure, which limits the accessible aqueous volume within and presents a barrier to the diffusion of larger molecules. Ultrastructural studies show that reassembly of the nucleus during telophase or late anaphase occurs by the close apposition of vesicles to condensed chromatin, followed by vesicle fusion (*13*). We suggest that an intact nuclear envelope,

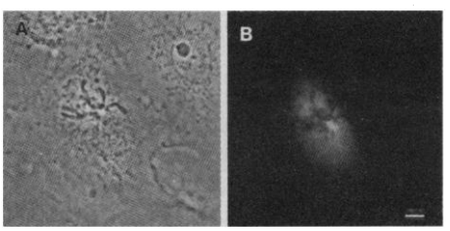

Fig. 3. Phase (**A**) and fluorescence (**B**) images of a mitotic PtK-2 cell loaded with FDx40. The cellular regions of excluded fluorescence in (B) correspond closely with the phase-dense chromosomes visible in (A). Scale bar, 10 μm.

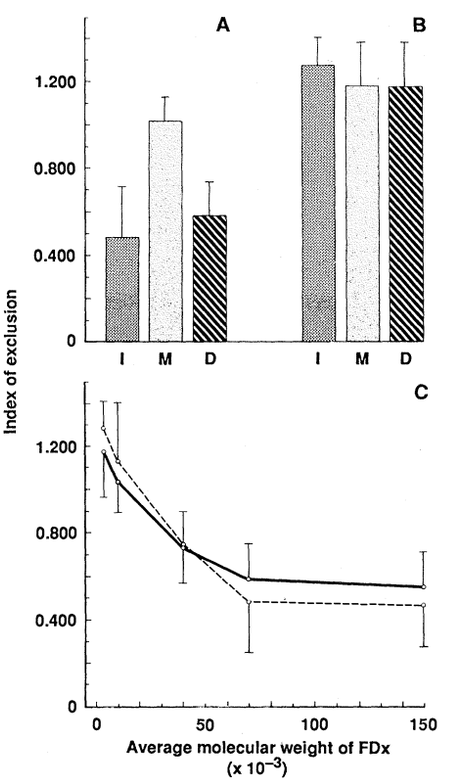

Fig. 4. Index of exclusion for FDx of various sizes in Swiss 3T3 cells. (**A**) Index of exclusion for cells loaded with FDx70 and TRDx10; I, interphase cells that had not divided since scratch-loading; M, mitotic cells; D, daughter cells. (**B**) Index of exclusion for cells loaded with FDx4 and TRDx10. The index value of slightly higher than 1.0 indicates concentration of FDx4 in the nucleus relative to TRDx10. (**C**) Index of exclusion for interphase cells loaded with TRDx10 and FDx of different average molecular weights. Dashed line, premitotic cells; solid line, postmitotic cells. Values represent the mean and standard deviation of 5 to 38 measured cells.

capable of excluding large macromolecules, is assembled around condensed chromatin before expansion, and that, therefore, the telophase nucleus encloses a sealed and soon to be expanded aqueous volume. The small aqueous space enclosed by the forming nuclear envelope would contain few dextran molecules. Large dextrans trapped in this small space would, according to this model, remain in the nucleus after its expansion but would be further diluted by nuclear expansion. Smaller dextrans would freely redistribute into the nucleus through the pores in the envelope.

In conclusion, our data identify a rapid, efficient, and size-selective mechanism by which large molecules can be excluded from the reassembling nucleus during mitosis. Although not all sufficiently large macromolecules would be expected to distribute similarly to dextrans (*4*), our data suggest that large, freely diffusible proteins would be excluded. We therefore propose that such exclusion might be among the earliest steps in reestablishing the interphase macromolecular identities of nucleoplasm and cytoplasm. Periodic access of cytoplasmic proteins to the nucleus, or the gradual accumulation of proteins in the nucleus of the postmitotic cell, could provide a novel mechanism for cell cycle–dependent gene regulation. Finally, the mechanism described here could periodically dilute soluble cytoplasmic proteins, such as tubulin (*3*), when nuclear envelope breakdown admits them into the nucleus, and then concentrate them during postmitotic expansion of the resealed daughter nuclei. Such concentration changes could consequently alter cytoplasmic architecture or metabolism.

REFERENCES AND NOTES

1. P. L. Paine and C. M. Feldherr, *Exp. Cell Res.* **74**, 81 (1972).
2. W. M. Bonner, *J. Cell Biol.* **64**, 431 (1975).
3. E. M. De Robertis, R. F. Longthorne, J. B. Gurdon, *Nature (London)* **272**, 254 (1978).
4. K. Luby-Phelps, F. Lanni, D. L. Taylor, *J. Cell Biol.* **102**, 2015 (1986).
5. P. L. Paine *et al.*, *Nature (London)* **254**, 109 (1975); R. Peters, *J. Biol. Chem.* **258**, 11427 (1983).
6. P. L. McNeil, R. F. Murphy, F. Lanni, D. L. Taylor, *J. Cell Biol.* **98**, 1556 (1984).
7. Cover slips containing subconfluent monolayers of cells were washed with warm, divalent cation-free phosphate-buffered saline (PBS), *p*H 7.4, then incubated briefly in 25 μl of PBS containing TRDx10 (5 mg/ml; Molecular Probes) and FDx (10 mg/ml) of one of several sizes: average molecular weight of 4,100 (FDx4), 10,000 (FDx10), 40,000 (FDx40), 70,000 (FDx70), or 150,000 (FDx150); Sigma Chemical Co.). These values are, according to their manufacturer, the number average molecular weight ± 5%. Cover slips were then scratched with jeweler's forceps, thus creating many "wounds" in the monolayer. After gentle rinsing with warm medium to remove unincorporated dextrans, cells were incubated for 24 hours at 37°C, by which time many of the cells had undergone mitosis.
8. G. J. Todaro, G. Lazar, H. Green, *J. Cell. Comp. Physiol.* **66**, 325 (1965); R. Dulbecco, *Nature (London)* **227**, 802 (1970).
9. Most cells on scratched cover slips were not fluorescent, as only a small percentage lined denuded zones, and cells that were loaded exhibited a wide range of fluorescence intensities (three orders of magnitude). This heterogeneity of fluorescence simplified identification of daughter cells, which, when derived from a loaded cell, exhibited fluorescence intensities similar to one another (within 10%). Other distinguishing characteristics of daughter cells were their rounded or mirror-image morphologies and their occasional residual connection by a cytoplasmic bridge. Fluorescence excitation in the microscope inhibited cell progression through mitosis, making it technically unfeasible to follow a single cell through mitotic division.
10. Fluorescence from cells was measured quantitatively by means of a photomultiplier (9558B, Thorn EMI); the current from it was amplified (current amplifier 427, Keithley) and displayed as a deflection on a chart recorder. The photomultiplier was coupled optically to a Zeiss photomicroscope and a 40× phase Neofluar (Zeiss) lens by means of a Zeiss photometer head equipped with an aperture that limited the measured region of fluorescence to a 5-μm-diameter spot size. This aperture was positioned over cell cytoplasm or nucleus by movement of the microscope stage. Then FDx and TRDx10 fluorescence were measured from the 5-μm spot by manual alternation of rhodamine and fluorescein filter sets (Zeiss). Background fluorescence, measured from a cell-free area of the microscope slide, was subtracted from cellular fluorescence. Background was never more than 10% of cellular fluorescence.
11. In positioning the photometric aperture over the nucleus, we collected fluorescence from nucleoplasm plus the cytoplasm above and below the nucleus. Our measurements underestimate the true ratio of FDx_{nuc} to FDx_{cyt}, as this would require a negligible volume of cytoplasm above and below the measured region of the nucleus.
12. C. M. Feldherr, *J. Cell Biol.* **31**, 199 (1966).
13. D. J. Fry, in *The Diversity of Membranes*, vol. 2 of *Mammalian Cell Membranes*, G. A. Jamieson and D. M. Robinson, Eds. (Butterworth, London, 1977), pp. 197–265; S. Ito, K. Dan, D. Goodenough, *Chromosoma* **83**, 441 (1981).

14. We thank E. Warder for technical assistance. Supported by grants from NIH (R23 CA44328 to J.S.; R01 CA42275 to P.M.), the American Cancer Society (CD 204 to P.M.), and the Whitaker Health Sciences Fund.

16 June 1987; accepted 24 August 1987

Technical Comments

Quick-Freeze Lipid Techniques: Correction

In my report "Lipid domains in fluid membranes: A quick-freeze differential scanning calorimetry study" (*1*), one of the lipids used, dipalmitoyl phosphatidylcholine (DPPC), was incorrectly labeled throughout the text as distearoyl phosphatidylcholine (DSPC) (*2*). Accordingly, figure 2A, a conventional scan of a mixture of pure dimyristoyl phosphatidylcholine (DMPC) bilayers and pure DPPC bilayers has two main endotherms with transition temperatures of 24°C (DMPC) and 42°C (DPPC). Figures 2B, 2D, and 2E are conventional scans of bilayers formed from a 1:1 molar mixture of DMPC and DPPC (DMPC-DPPC bilayers). These scans show, as expected, one major endotherm characteristic of bilayers formed from a mixture of these two lipids.

Unlike the conventional scans of DMPC-DPPC bilayers, the quick-freeze scan, figure 2C, shows two separate endotherms. Unlike conventional scans of pure DMPC bilayers or pure DPPC bilayers, no pretransitions are observed. The onset temperatures of the two endotherms seen in the quick-freeze scan are approximately the same (19° and 44°C) as those of the main transitions of pure DMPC and DPPC. The endotherms observed in the quick-freeze scan of the DMPC-DPPC bilayers are, however, substantially broader and differ in shape from those observed by conventional calorimetry on bilayers composed of the individual lipid species (figure 2A). Although the higher temperature endotherm seen in figure 2C begins at about 44°C, heat absorption is not complete until approximately 63°C. Since the transition temperature of pure DSPC bilayers is 55°C, the temperature range of the higher temperature endotherm seen in figure 2C makes the error in labeling DPPC as DSPC less obvious. I regret any confusion this may have caused.

It should be emphasized that for bilayers formed from a single lipid species, our quick-freeze techniques have never given samples whose calorimeteric behavior differed from that of conventional preparations. The major finding illustrated in figure 2 is, therefore, that quick-freeze methodology applied to DMPC-DPPC bilayers gives thermograms that differ from those obtained by conventional differential scanning calorimetry (DSC) on this mixture. The two peaks obtained for DMPC-DPPC bilayers by quick-freeze DSC also differ from those for pure bilayers of either DMPC or DPPC.

DONALD L. MELCHIOR
Department of Biochemistry, University of Massachusetts Medical School, Worcester, MA 01655

REFERENCES AND NOTES

1. D. L. Melchior, *Science* **234**, 1577 (1986).

2. I would like to thank Michael A. Singer and Leonard Finegold for pointing out the labeling error.

11 August 1987; accepted 12 August 1987